

## Non-linear dynamics of cardiac excitation and impulse propagation

Dante R. Chialvo & Jose Jalife\*

Department of Pharmacology, SUNY Health Science Center at Syracuse, Syracuse, New York 13210, USA

Extremely complex frequency-dependent patterns of excitation and impulse propagation can be shown in cardiac tissues. Such complex behaviour can be analysed using methods derived from chaos theory<sup>1-4</sup>, which is concerned with the non-linear dynamics of deterministic systems that have irregular periodicities as well as an exquisite sensitivity to the initial conditions. We report here that the general response patterns of non-oscillatory cardiac conducting tissues, when driven rhythmically by repetitive stimuli from their surroundings, are similar to those of other deterministic systems showing chaotic dynamics. Such patterns include phase locking, period-doubling bifurcation and irregular activity. We have used electrophysiological techniques and analytical arguments to explain this unforeseen behaviour and to provide some key information about its mechanisms. The study of these dynamics is of general application to the understanding of disordered phenomena in excitable media, and may provide new insight about the origin of fatal cardiac arrhythmias.

Chaos theory focuses on the analysis of a behaviour that, while apparently random, has limited boundaries and can be quite stable. On the other hand, the term 'chaotic' has been used by cardiac electrophysiologists to describe fibrillatory cardiac

activity in which excitation occurs in a seemingly random and unpredictable fashion<sup>5</sup>. Recent studies<sup>6</sup> of cardiac tissues have shown some forms of irregular dynamics that resemble those observed in other deterministic systems<sup>7-9</sup>. Indeed, phase locking and period doubling have been shown in aggregates of embryonic heart cells undergoing self-sustaining pacemaker activity<sup>10</sup>. No previous experimental attempt, however, has been made to show locking phenomena and irregular dynamics in excitable non-pacemaker cardiac tissues.

Our studies were conducted in two groups of experiments. In the first group, ten quiescent Purkinje fibres from sheep were used to determine the quantitative aspects of the response patterns to external stimuli. Preparations were driven with depolarizing current pulses applied through a suction pipette. Recordings were obtained in each experiment to construct steady-state strength-duration curves for various basic cycle lengths (BCLs) and stimulus-response ratios (SRRs). For each curve (Fig. 1a), each data point obtained at a given duration and BCL was defined as the minimal current strength at which a stable SRR was maintained. If the stimulus-response pattern repeated periodically, the SRR was termed to be 'phase-locking' or, more accurately, 'parameter-response locking'. As shown in Fig. 1a, obtained at a BCL of 700 ms, any point falling on or above the 1:1 curve would give rise to 1:1 SRR (that is, each stimulus would be followed by one action potential). At BCLs longer than those shown in Fig. 1, the only parameter-response locking observed below 1:1 was 1:0. But as shown in Fig. 1a, (BCL = 700 ms), when the BCL was decreased to the range between 1,000 and 230 ms, the 1:1-1:0 boundary became wider, and other locking patterns emerged at intermediate levels of current strength. A more complete picture of these patterns is shown in Fig. 1b. Several different parameter-response locking regions are presented. The lines are the limits of the most important isoperiodic areas (1:1, 2:1, 3:1 and 1:0) found in

\* To whom correspondence should be addressed.

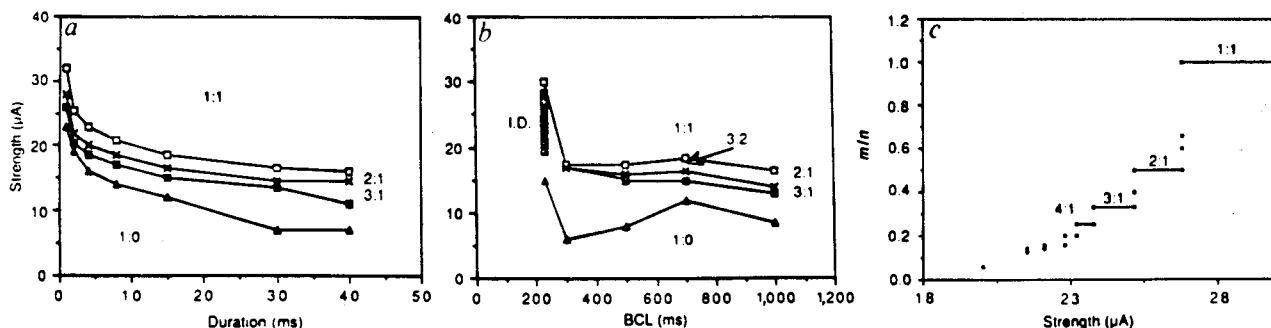


Fig. 1 a, Steady-state strength-duration curves of a Purkinje fibre from a sheep. Repetitive depolarizing-current pulses at a BCL of 700 ms. For each duration, current strength was decreased in steps of 1-2  $\mu\text{A}$  beginning at levels of 1:1 locking. Symbols on each of the top three curves indicate the minimum current strength for a given pattern: open squares, 1:1; crosses, 2:1; closed squares, 3:1. Additional locking patterns between 3:1 and 1:0 (closed triangles) are not shown for simplicity. b, Parameter plane from the same experiment as in a for 15 ms-pulses at BCLs of 1,000, 700, 500, 300 and 230 ms. Curves and symbols indicate the limits of the most important isoperiodic areas (1:1, 2:1, 3:1 and 1:0). Other locking patterns occurred within very narrow regions; for instance, 3:2 locking (arrowed) between 1:1 and 2:1. The stippled area corresponds to the region of irregular dynamics. The pattern was considered to be 1:0 when, after a single action potential was initiated, at least 100 subsequent stimuli were not followed by a response. c, 'Devil's staircase'<sup>24</sup> from one Purkinje-fibre experiment. The response-to-stimulus ratio ( $m/n$ ) is plotted as a function of the current strength, which was decreased in very small steps. Pulse duration and BCL were fixed at 10 and 600 ms, respectively. Beginning at 28.0  $\mu\text{A}$ , 1:1 locking ( $m/n = 1.0$ ) persisted until 26.9  $\mu\text{A}$ , at which point 3:2 locking ( $m/n = 0.66$ ) appeared. A very small ( $<0.1 \mu\text{A}$ ) decrease in strength, however, resulted in a 5:3 pattern. At 26.8  $\mu\text{A}$ , 2:1 locking ( $m/n = 0.5$ ) was established. Further decreases in current strength yielded stable 'steps' of  $m/n$  of 0.33-0.059. If the mid-values of steps 2:1, 3:1...  $n+1:1$  were connected, the resulting function would be described by the equation:  $\text{strength} = (18.7 + (25.7/(1/n))) - (23.1/(1/n)^2)$ ;  $R = 1.00$ .

**Methods.** Cardiac Purkinje fibres were dissected from the hearts of young sheep (10-25 Kg) anaesthetized with sodium pentobarbital (35 mg per Kg). Thin, externally-unbranched false tendons (outer diameter, 0.4-0.6 mm; length  $>10$  mm) were placed in warm, oxygenated (95%  $\text{O}_2$ , 5%  $\text{CO}_2$ ) Tyrode solution of the following composition (mM): NaCl, 130;  $\text{NaHCO}_3$ , 24;  $\text{NaH}_2\text{PO}_4$ , 1.2;  $\text{MgCl}_2$ , 1.0;  $\text{CaCl}_2$ , 1.8; KCl, 4.0 and glucose, 5.6. The pH was 7.4. Group 1. Preparations were placed in a tissue bath (5 ml) and superfused with oxygenated Tyrode solution at 32  $^\circ\text{C}$ . At this low temperature, the ranges of the various parameter-response locking patterns were greatly amplified. Fibres were driven rhythmically by the application of constant current depolarizing pulses, delivered by a modified P6i Frederick Haer stimulator (Haer) through a suction pipette (outer diameter, 0.3 mm) at various BCLs. Current strength was measured continuously as the voltage drop across a 1 k $\Omega$  resistor in series with the suction pipette. Transmembrane potentials were recorded with a glass microelectrode filled with 3 M KCl (d.c. resistance 10-30 M $\Omega$ ), connected to a high input impedance amplifier (Model 750, WP Instruments). Signals were displayed on a digital oscilloscope (Tektronix 5222) and recorded on analog tape (Model D, Vetter) for later analysis.

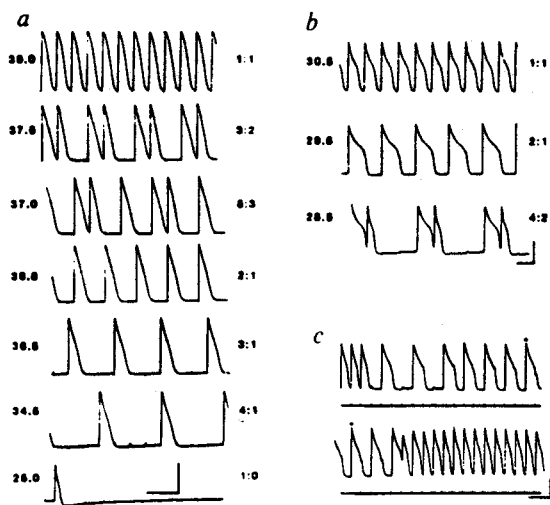


Fig. 2 Phase locking, period doubling and recurrent fluctuations in excitation of a Purkinje fibre. *a*, Transmembrane potentials obtained when current strength was decreased gradually from 39 (1:1 locking; uppermost trace) through 25  $\mu\text{A}$  (1:0 locking; bottom trace). Various other patterns (not shown) occurred between 4:1 and 1:0. After the last action potential at 25  $\mu\text{A}$ , no activity was manifest even during more than the 12 s of continuous recording shown here. Numbers at left indicate current strength in  $\mu\text{A}$ ; numbers at right denote parameter: response ratios. Pulse duration, 5 ms; BCL, 300 ms. Vertical calibration is 60 mV for all traces; horizontal calibration is 600 ms for all, except bottom trace (1,500 ms). *b*, Analog recordings from a different experiment (pulse duration, 15 ms; BCL, 600 ms). At 30.5  $\mu\text{A}$ , 1:1 was present. This was followed by 2:1 at 29.5  $\mu\text{A}$ . Further decreasing the current strength to 28.5  $\mu\text{A}$ , however, led directly to a 4:2 locking pattern, and not to the expected 3:1. Calibrations are: vertical, 60 mV; horizontal, 60 ms. Numbers on right and left of traces are same as in *a*. *c*, Recurrent fluctuations in the activity in the same fibre as in *b* (pulse duration, 20 ms; strength, 41  $\mu\text{A}$ ; BCL, 500 ms). A stimulus monitor is shown below each trace. The last action potential (diamond) on top panel of *c* is reproduced at the beginning of bottom panel. At constant pulse magnitude and BCL, 1:1 locking is present during the first three beats. But the fourth stimulus fails to initiate a response, which leads to various unstable patterns until 1:1 is reestablished. This behaviour repeated periodically after every 40 to 50 beats. Note large prolongation of action potential duration during fourth response. Calibrations: vertical 50 mV; horizontal 1,000 ms.

this representative preparation. The largest area between 1:1 and 1:0 was 2:1, between 1:0 and 2:1 was 3:1, between 3:1 and 1:0 was 4:1, and so on. Several forms of Wenckebach-like patterns<sup>11</sup> were also manifest. Curiously, these patterns were found in areas that were proportionately narrower than those between 1:0 and 2:1. Consequently the most commonly observed stable locking of this kind was 3:2 (arrowed in Fig. 1*b*), whereas others (for example 4:3 and 5:4) were seen as unstable patterns between 1:1 and 3:2 or 2:1.

Certain types of parameter-response locking occurred within relatively narrow areas of stimulus strength and BCL. For example, 5:3 locking could be manifest as an alternation between 2:1 and 3:2 (see Fig. 2*a*). In fact, the overall hierarchy follows the so-called Farey sequence that is universally observed in oscillatory systems<sup>12,13</sup>. Hence, within a given range of BCLs, the largest area between  $n:m$  and  $N:M$  was always  $n+N:m+M$ ; where  $n$  and  $N$  are the number of pulses and  $m$  and  $M$  the number of responses. Thus, our data show that this structure is not restricted to self-sustaining oscillators, which was predicted by previous theoretical and experimental studies<sup>14-19</sup>.

Interestingly, the periodic patterns we have observed in all our experiments adhere also to another well-known universal

rule<sup>20-22</sup>—if in a given sequence of stimulation we define successful activation as 1 and failure as 0, the periodic pattern 1,1,0,1,0 (5:3 locking) will be found only between areas of 1,1,0 (3:2 locking) and 1,0 (2:1 locking), which is true also for longer sequences, depending on the amount of experimental noise acting to destroy such sequences. These observations suggest that, when the pulse parameters are changed, it is possible to predict the locking period (for example 2:1, 3:1, and so on following Farey's series) as well as the order of action potentials and dropped beats within a given sequence.

The experimental data presented in Fig. 1*c* show the scaling properties of the behavioural structure. In this case, the action potential ( $m$ ) to stimulus ( $n$ ) ratio is plotted as a function of the pulse strength. Clearly, the plot resembles the 'devil's staircase' of phase locking in oscillatory systems<sup>23</sup>. In a strict sense, however, if such a scaling behaviour is predictable as in other deterministic systems<sup>24</sup>, a function joining the mid-values of the steps 2:1, 3:1...  $n+1:1$  should be close to a power law of 2. Analysis of our results confirmed the existence of that function.

The hierarchical structure described above was lost at values of BCL and strength such as those within the stippled area of Fig. 1*b*. In this region, we found irregular dynamics (ID) coexisting with parameter-response locking. Normally, when 1:1 locking was lost as pulse strength was decreased in small steps, the sequence of stable phase-locking patterns was 3:2, 5:3, 2:1, 3:1, 4:1, ... 1:0 (Fig. 2*a*). But in some cases, lowering the stimulus strength changed the pattern from 1:1 directly into 3:1 or 4:1 rather than the expected 2:1. In other cases, such as that illustrated in Fig. 2*b*, decreasing the current-pulse strength in very small steps from the 1:1 domain yielded the sequence 1:1  $\rightarrow$  2:1  $\rightarrow$  4:2. This can be regarded as a period-doubling bifurcation as has been described in other systems<sup>1</sup>. Other more typical examples of period-doubling bifurcation are also present, including a 2:2 pattern in which a stimulus is always followed by an action potential whose amplitude, duration or latency (see Fig. 3*a*) alternates on a beat-to-beat basis.

In yet other cases, we found recurrent fluctuations in the behaviour. Indeed, as shown in Fig. 2*c*, under some accurately controlled conditions of fixed stimulus magnitude and BCL, 1:1 locking was lost and the sequence became: 1:1... 2:1  $\rightarrow$  3:1, 3:1  $\rightarrow$  2:1... 2:1  $\rightarrow$  1:1... 2:1  $\rightarrow$  3:1 and so on. Three different frequencies coexist during this activity: the frequency of stimulation, the frequency of the fibre response and the frequency of repetition of the overall behaviour. In our experiments, this particular type of activity may have depended on at least two dynamical factors. First, the fibres must have had supernormal excitability at very early intervals<sup>25</sup>, and second, the prolongation of the action potential duration after the first dropped beat must have occurred rapidly. Similar dynamics were found also near other stable phase-locking regions (for instance, 2:1 and 3:1), suggesting that recurrent fluctuation 'surrounds' the stable parameter-response locking regions.

The strength versus BCL plot of Fig. 1*b* can be considered as the parameter plane of our non-linear system. In such a plane, the irregular dynamics are more often observed within narrow regions at the upper-left margin, rather than at the lower phase-locking regions. Parameter-space analysis has shown that non-linear driven oscillators also show this proportionality<sup>26,27</sup>.

In a second group of eight experiments, the dynamic behaviour of our preparations was studied as a spatial phenomenon during action-potential propagation along a linear non-homogeneous cell strand. In this case, the parameters that were used to induce the various dynamics were changes in the BCL and in the effective conduction velocity along the strand. Unbranched, quiescent Purkinje fibres from sheep were placed in a three-chambered tissue bath<sup>28</sup> and driven by surface stimuli applied at one end of the fibre. Effective conduction velocity was measured between two microelectrodes, one proximal (P) and the other distal (D) to the stimulating electrode. When all three segments were superfused with normal Tyrode, impulses

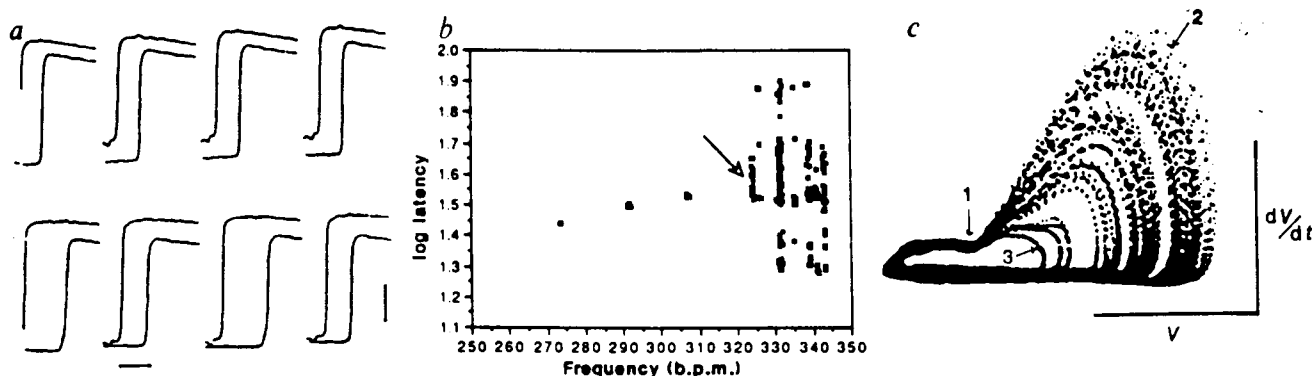


**Fig. 3** *a*, Period doubling of cardiac impulse propagation. In both panels, the top trace is proximal (P), and bottom trace is distal (D) action potential recording from a linear Purkinje fibre placed in a three-chamber bath<sup>28</sup>. The top panel shows frames (duration 6 ms) of four consecutive beats at a BCL of 212 ms. P-D latency was consistent. A similar sequence is shown in the bottom panel at a BCL of 208 ms. In this case, P-D latency alternated between 1.6 and 2.9 ms. P-D distance, 6.2 mm. Conduction velocity at BCL, 1,000 ms was relatively slow ( $4.4 \text{ m s}^{-1}$ ) because of slight compression on the fibre by the two rubber membranes bounding the central chamber (1.5 mm). Calibrations: vertical, 40 mV; horizontal, 2 ms. *b*, Irregular dynamics following period doubling of P-D latency in a three-chamber bath experiment. Abscissa, P frequency; ordinate, log of P-D latency. P-D latency increased monotonically as frequency was increased. Latency doubling began to occur at the critical value of 322 b.p.m. (arrow), with the 'arms' of the bifurcation separating gradually as the frequency was further increased. Irregular dynamics developed between 325 and 345 b.p.m. During more than 100 beats in which irregular dynamics were recorded, the sequence of latencies was always long-short-long, and so on. Note that certain intermediate values of P-D latency were never recorded. *c*, Phase plane trajectories ( $V$  = membrane potential;  $dV/dt$  = first derivative of membrane potential) of the D cell, taken from the same experiment as in *b* during irregular dynamics at 332 b.p.m. Inter-electrode distance, 8.7 mm; heptanol (1.5 mM) superfusion in central chamber (1.48 mm in length); P-D latency at BCL = 1,000, 4.0 ms (conduction velocity,  $2 \text{ m sec}^{-1}$ ). Calibrations: vertical,  $200 \text{ V s}^{-1}$ ; horizontal, 40 mV.

**Methods.** Group 2. A three-compartment bath<sup>28</sup> was used for these experiments. The fibres were threaded through the holes of two latex membranes that bounded the central chamber of the bath, and were superfused with Tyrode solution at  $37^\circ\text{C}$ . Preparations were driven through a pair of surface bipolar electrodes on one end of the fibre. Transmembrane potentials were recorded simultaneously with two microelectrodes, each located in one of the outer chambers. All signals were amplified, monitored and stored as described for Group 1 (see Fig. 1 legend). For all experiments, data were analysed by playing back the tape-recorded signals on the digital oscilloscope through a low-pass filter, and sending them to an analog X-Y plotter (Omnigraphic, Houston Instruments). Latency versus frequency plots (see Fig. 3*b*) were constructed also directly from the tape-recorded signals. P-P intervals and P-D latencies were measured with an input-output and A-D conversion module (models 64IF22 and 64IF/ADC0816, Schnedler Systems, Inc.) interfaced with a microcomputer (Commodore C128). Zero voltage crossing of the P or D signal started and stopped the computer clock (precision  $10 \mu\text{s}$ ). Phase-plane trajectories were obtained off-line by feeding the recorded voltages into an analog differentiator (linear between 1 and  $500 \text{ V s}^{-1}$ ), and plotting the resulting signal against voltage on the digital oscilloscope. Variable external sampling rate (faster during the upstrokes, slower during repolarization) was used to save oscilloscope memory (limit, 1,024 samples), thus allowing the superposition of about 100 trajectories on each frame.

initiated at a frequency of 1 per s propagated in a one-to-one manner, with conduction velocities greater than  $5 \text{ m s}^{-1}$ . Stimulation at increasing rates led to a progressive increase in P-D conduction time (latency), until the pattern evolved directly and predictably into 2:1. When the central segment (1–2 mm long) was slightly compressed or superfused with 1.25 to 1.5 mM of the electrical uncoupler heptanol<sup>29</sup>, 1:1 conduction at a rate of 1 per s became slower than in the control. At intermediate levels of conduction impairment (with a conduction velocity of 5 to  $1.5 \text{ m s}^{-1}$ ), stimulation at increasing rates also led to a progressive increase in P-D latency, until 2:1 locking occurred. Under these conditions, however, the 2:1 pattern was preceded by period doubling. Figure 3*a* shows an example. Oscilloscope tracings of four consecutive P and D action potentials are shown in each panel during the initial 6 ms after the corresponding stimulus. In the upper panel, at a BCL of 212 ms, 1:1 locking was observed with a constant P-D latency of 1.7 ms. As the BCL was reduced in 1 ms steps, the P-D latency began to alternate on a beat-to-beat basis, with a gradual increase in the difference between brief and long latencies. In the lower panel, at a BCL of 208 ms, P-D latency alternated between 1.6 and 2.8 ms.

Figure 3*b* shows the results of a more complete experiment in which the first period-doubling bifurcation (2:2) was followed by more irregular dynamics, before 2:1 locking occurred. The P-D latency (ordinate) is plotted as a function of the driving frequency (abscissa). Clearly, as the driving rate was increased, P-D latency also increased until, at 322 beats per min (b.p.m.), a bifurcation was reached (arrow) at which long and brief

latencies began to alternate. From this point on, all increments in pulse frequency were made in  $1 \text{ ms}^{-1}$  steps and at least 100 beats were plotted for each step. The period was 2 between the initial bifurcation and 325 b.p.m., where latency again became unstable. Higher periodicities began to emerge as the frequency changed from 330 to 345 b.p.m. Even though, under these conditions, the variation in latency was large and complex, it was not random, as certain values of latency were never visited. This suggests a chaotic structure<sup>30</sup>.

The results in Fig. 3*c* are presented in the form of phase-plane trajectories. One hundred responses are plotted at a driving rate of 332 b.p.m. Two important dynamical features are shown by this experiment. The first one, already alluded to in the latency domain, is that some orbits are never visited, as is clear by the structure of the state-space portrait (Fig. 3*c*). The second one is a didactic example of the property known as 'sensitive dependence on the initial conditions'. During the  $n$ th beat, the state variables (membrane voltage,  $V$ , and  $dV/dt$ ) are in the sub-threshold excursion represented by point 1. Ten milliseconds later, the state variables have moved to point 2. In the next beat ( $n+1$ ), the variables are again very close to, but not precisely at point 1. As a consequence of this small difference in the initial conditions, there is a strong divergence in the subsequent trajectory which, after 10 ms, leads the state variables to point 3. This behaviour is very similar to that described for other deterministic systems that show chaotic dynamics<sup>31</sup>.

Finally, in these experiments, when the degree of conduction impairment induced by segmental compression or by superfusion with heptanol was high (conduction velocity  $< 1.5 \text{ m s}^{-1}$

at BCL = 1,000 ms), various sequences of parameter-response locking were found as the driving frequency was changed. These sequences were very similar to those described for the first group of experiments, and also followed Farey's universal progression of phase-locking patterns.

In conclusion, parameter-response locking, irregular dynamics and chaotic-like behaviour can occur in cardiac Purkinje fibres that do not undergo spontaneous activity. This may have important implications from the theoretical as well as from the experimental and clinical points of view. Theoretically, the surprising behaviour of our preparations raises two open questions directed to mathematicians and theoretical physicists. Is self-sustaining oscillation fundamental to the demonstration of chaotic dynamics? If not, can the chaotic dynamics of a non-oscillatory system that follow universal rules be described by the same theoretical techniques<sup>32,33</sup> as those used in the analysis of driven non-linear oscillators? For the

experimental and clinical cardiologist, the implication of such dynamics for the study of cellular mechanisms of cardiac-rhythm disturbances and for the development of sudden cardiac death<sup>34</sup> is extremely interesting and deserves to be explored. Nonlinear dynamics has helped to suggest new experimental approaches in the analysis of normal electrophysiology of the heart and its alterations<sup>35</sup>. By focusing on these properties it might be possible to reach an understanding of the mechanisms of a number of rate-dependent conduction disturbances<sup>36,37</sup>. By utilizing biological models of cardiac electrical activity to study the transition from regular to irregular (chaotic?) dynamics, new insight might be gained into the origin of erratic, sometimes fatal arrhythmias observed in the clinic.

This work was supported by the NIH. We thank D. C. Michaels, M. Delmar and J. Anumonwo for helpful discussions, P. Chiale for his help in some of the experiments, and O. Piro for sharing his unpublished data with us.

Received 28 August; accepted 29 October 1987.

- Holden, A. V. *Chaos* (Princeton University Press, 1986).
- Cvitanovic, P. *Universality in Chaos* (Hilges, Bristol, 1984).
- Hao, B.-L. *Chaos* (World Scientific, Singapore, 1984).
- Devaney, R. L. *An Introduction to Chaotic Dynamical Systems* (Benjamin Cummings, Menlo Park, 1986).
- Moe, G. K., Rheinboldt, W. C. & Abildskov, J. A. *Am. Heart J.* **67**, 200-220 (1964).
- Guevara, M. R., Glass, L. & Shrier, A. *Science* **214**, 1350-1353 (1981).
- Simoyi, R. H., Wolf, A. & Swinney, H. L. *Phys. Rev. Lett.* **49**, 245-248 (1982).
- Gollub, J. P. & Benson, S. V. *J. Fluid Mech.* **100**, 449-470 (1980).
- Testa, J., Perez, J. & Jeffries, C. *Phys. Rev. Lett.* **48**, 714-717 (1982).
- Glass, L., Shrier, A. & Belair, J. in *Chaos* (ed. Holden, A.) 237-256 (Princeton University Press, 1986).
- Zipes, D. P. *Circulation* **60**, 465-472 (1979).
- Arnold, V. I. *Geometrical Methods in the Theory of Ordinary Differential Equations. Section II* (Springer, New York, 1983).
- Glass, L. & Perez, R. *Phys. Rev. Lett.* **48**, 1772-1775 (1982).
- Guevara, M. R., Ward, G., Shrier, A. & Glass, L. *Comp. Cardiol.* **11**, 167-170 (1984).
- Feingold, M., Gonzalez, D., Piro, O. & Viturro, H. *Phys. Rev. Lett.* (submitted).
- Harmon, L. P. *Kybernetik* **1**, 89-101 (1961).
- Guttman, R., Feldman, L. & Jakobsson, E. *J. Membrane Biol.* **56**, 9-18 (1980).
- Glass, L., Guevara, M. R. & Shrier, A. *Ann. N.Y. Acad. Sci.* **584**, 168-178 (1987).
- Matsumoto, G. *et al. Phys. Lett. A* **123**, 162-166 (1987).
- Sato, S. *Kybernetik* **11**, 208-216 (1972).
- Nagumo, J. & Sato, S. *Kybernetik* **10**, 155-164 (1972).
- Yoshizawa, S., Osada, H. & Nagumo, J. *Biol. Cybern.* **45**, 23-33 (1982).
- Mandelbrot, B. B. *The Fractal Geometry of Nature* (Freeman, San Francisco, 1982).
- Kaneko, K. *Collapse of Tori and Genesis of Chaos in Dissipative Systems* (World Scientific, Singapore, 1986).
- Spear, J. F. & Moore, E. N. *Circulation Res.* **35**, 782-792 (1974).
- Gonzalez, D. & Piro, O. *Phys. Rev. Lett.* **50**, 870-872 (1983).
- Guevara, M. R. & Glass, L. *J. Math. Biol.* **14**, 1-23 (1982).
- Jalife, J. & Moe, G. K. *Circulation Res.* **39**, 801-808 (1976).
- Johnston, M. F., Simon, S. A. & Ramon, F. *Nature* **286**, 498-500 (1980).
- Rapp, P. E. *et al. in Lecture Notes in Biomathematics 66. Nonlinear Oscillations in Biology and Chemistry* 175-205 (1986).
- Vidal, C. in *Nonlinear Phenomena in Chemical Dynamics* (eds Vidal, C. & Pacault, A.) 49-62 (Springer, Berlin, 1981).
- Guckenheimer, J. *IEEE Trans. Circuits and Systems* **30**, 586-591 (1983).
- Borenblatt, G. I., Ioos, G. & Joseph, D. *Nonlinear Dynamics and Turbulence* (Pitman, London, 1983).
- Ritzenberg, A., Adam, D. & Cohen, R. *Nature* **307**, 159-161 (1984).
- Winfree, A. T. *When Time Breaks Down. The Three-Dimensional Dynamics of Electrochemical Waves and Cardiac Arrhythmias* (Princeton University Press, 1987).
- Rosenbaum, M. B., Elizari, M. V., Levi, R. J. & Nau, G. J. *Chest* **63**, 678-688 (1973).
- Halpern, M. S., Nau, G. J., Chiale, P. A., Elizari, M. V. & Rosenbaum, M. B. in *Frontiers of Cardiac Electrophysiology* (eds Rosenbaum, M. B. & Elizari, M. V.) 465-487 (Nijhoff, The Hague, 1983).